

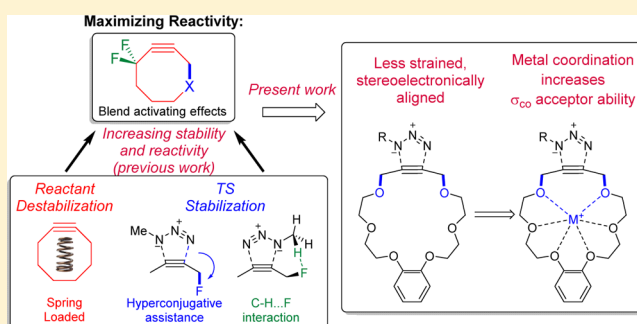
# Alkynyl Crown Ethers as a Scaffold for Hyperconjugative Assistance in Noncatalyzed Azide–Alkyne Click Reactions: Ion Sensing through Enhanced Transition-State Stabilization

Brian Gold, Paratchata Batsomboon, Gregory B. Dudley,\* and Igor V. Alabugin\*

Department of Chemistry and Biochemistry, Florida State University, Tallahassee, Florida 32306-4390, United States

**S** Supporting Information

**ABSTRACT:** Our recent work has provided an alternative strategy for acceleration of azide/alkyne cycloadditions via selective transition state (TS) stabilization. Optimization of hyperconjugative assistance, provided by the antiperiplanar arrangement of propargylic  $\sigma$ -acceptors relative to the forming bonds, is predicted to relieve strain in cyclooctynes while providing large acceleration to the cycloaddition. The present work investigates this strategy in alkynyl crown ethers, where propargylic C–O bonds contained within the macrocycle are constrained close to proper alignment for hyperconjugative assistance. Preorganization of  $\sigma$ -acceptors into the optimal arrangement for hyperconjugative interactions may alleviate a portion of the entropic penalty for reaching the TS. Optimal alignment can be reinforced, and transition-state stabilization can be further amplified by binding positively charged ions to the crown ether core, highlighting the potential for applications in ion sensing.



## INTRODUCTION

“Click chemistry”<sup>1</sup> is revolutionizing the molecular sciences, with applications ranging from drug design<sup>2</sup> and chemical biology<sup>3</sup> to materials science,<sup>4</sup> development of sensors,<sup>5</sup> and polymer chemistry,<sup>6</sup> among others. In vivo applications<sup>7</sup> of the prototypical “click reaction”,<sup>8</sup> the copper-catalyzed variant<sup>9,10</sup> of the Huisgen azide–alkyne cycloaddition (CuAAC),<sup>11</sup> are limited by the toxicity of copper salts.<sup>12</sup> CuAAC also presents a problem in the functionalization of quantum dots and other nanomaterials, as the copper salts negatively impact the luminescent properties of nanocrystals.<sup>13,14</sup>

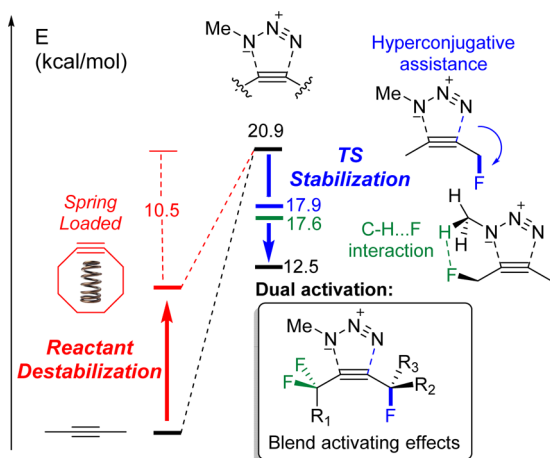
Metal-free alternatives to the CuAAC provided by Bertozzi,<sup>15</sup> Boons,<sup>3b,16</sup> and others<sup>17</sup> have harnessed the “explosive reactivity” of activated cyclooctynes (OCT) in strain-promoted<sup>18</sup> azide–alkyne cycloadditions (SPAAC). These advances have allowed for intracellular azide–cyclooctyne coupling within hours at room temperature,<sup>3a,19</sup> enabling in vivo biological imaging<sup>20</sup> and ultimately spawning a new field of bioorthogonal chemistry.<sup>7</sup> Still in the early stages of development, bioorthogonal techniques provide new methods for the study of biological processes. Such studies often utilize azide-functionalized sugars, etc., which can be incorporated into biomolecules via natural metabolic pathways.<sup>21</sup> The advantages provided by rapid reaction kinetics prompted the efforts to “brush against the line between stability and reactivity without crossing it,” where lactam-based biarylcyclooctyne (BARAC) provides a 10-fold increase in reactivity over dibenzocyclooctyne (DIBO), leading to intracellular coupling within minutes.<sup>22</sup>

The initial breakthroughs in SPAAC, discussed above, clearly illustrate the utility of reactant destabilization in the design of reactive alkynes.<sup>23</sup> While strain activation has provided access to an arsenal of options for bioorthogonal applications, this approach cannot escape the inherent drawback of relatively unstable compounds, enhancing the reactivity at the cost of reactant ground-state stabilization. Glimpses of an alternative strategy, transition-state stabilization, appeared when Bertozzi et al. observed the reactivity of OCT can be enhanced >50-fold by incorporation of fluorine atoms at the propargylic position in difluorocyclooctyne (cf. DIFO).<sup>24</sup> The  $\sim 2$  kcal/mol decrease in the activation barrier for DIFO relative to cyclooctyne is reproduced by DFT computations,<sup>25</sup> yet specific orbital interactions and an understanding needed in order to fully utilize such an approach remained elusive until recently.<sup>26</sup>

In our previous work, we were able to identify precise stereoelectronic interactions responsible for selective TS stabilization (Figure 1). Acceleration is provided via hyperconjugative assistance for 1,4-addition and a CH...F interaction for 1,5-addition. The stereoelectronic nature of such TS stabilization<sup>27</sup> is revealed by the observation that a single antiperiplanar propargylic fluorine substituent in the acyclic substrate (1-fluorobut-2-yne) is greater than the TS stabilization provided by two gauche fluorines in DIFO.<sup>26</sup> The judicious placement of activating substituents becomes apparent in the recent analysis of electronic effects on BARAC, where the most

Received: May 1, 2014

Published: June 13, 2014



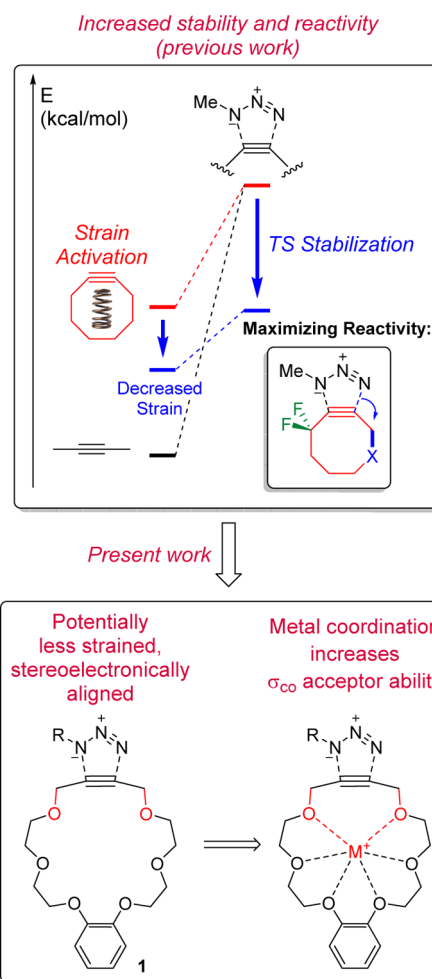
**Figure 1.** Comparison of alternative strategies for acceleration of copper-free click reactions, reactant destabilization (red), and TS stabilization (blue). TS stabilization can be provided via hyperconjugative (blue) or C–H...F H-bonding interactions (green). The efficiency of synergistic transition state stabilization in 1,1,4-trifluoro-2-butyne approaches reactant destabilization in OCT. Activation energies calculated at the B3LYP/6-31G(d) level of theory, energies in kcal/mol.<sup>26</sup>

dramatic observed remote substituent effect, due to double fluorine-substitution, was a rate enhancement only  $\sim 2$  times the parent compound ( $0.9 \rightarrow 1.6 \text{ M}^{-1} \text{ s}^{-1}$ ).<sup>28</sup>

In linear systems, propargylic acceptors provide TS stabilization in two ways: (a) a decrease in the alkyne distortion energy (the energy cost for alkyne bending needed to reach the cycloaddition TS geometry) and (b) assistance to the bond formation. The alkyne  $\pi$ -bond becomes a better donor upon bending, increasing the hyperconjugative interactions, but another interaction manifests itself as the azide approaches. The filled frontier orbital of the azide mixes with the alkyne LUMO, partially redirecting electron density to the alkyne  $\pi^*$ .<sup>25b,29,30</sup> This interaction is facilitated by appropriately positioned propargylic  $\sigma^*$  or  $\pi^*$  acceptors, assisting in the C...N bond formation.<sup>31</sup> Both of these interactions increase leading into the transition state, thereby providing selective cycloaddition TS stabilization. The stereoelectronic nature of this interaction renders it imperfect in DIFO but allows for full manifestation when the  $\sigma$  acceptor is antiperiplanar (app).

A complementary C–H...F contact, which can be considered a H-bond with a significant electrostatic component (Figure 1), can be utilized in addition to hyperconjugative assistance. When combined, these two independent mechanisms provide an even larger acceleration once additional  $\sigma$ -acceptors are introduced. Remarkably, the proper positioning of just three C–F bonds at the propargylic carbons eliminates  $\sim 80\%$  of the barrier difference between 2-butyne and cyclooctyne without introducing strain destabilization in the reactant.

In cyclic alkynes containing propargylic acceptors, the TS stabilization provided by assistance to alkyne bending is less important than in linear systems (the TS is only slightly more bent than the cyclic starting material), and the main factor responsible for rate enhancement relative to alkynes activated by strain alone is the assistance to bond formation.<sup>32</sup> In fact, propargylic acceptors stabilize bent alkynes by relieving strain (Figure 2), which can be counterproductive toward reactivity, unless hyperconjugative interactions increase in the transition state (i.e., assistance to bond formation).<sup>33</sup> Our predictions



**Figure 2.** Theoretical basis for TS stabilization studied in the present work. Strategies for activation are color-coded according to Figure 1.

suggest that by combining the optimized TS stabilizing effects with strain, alkynes that are actually less strained than those currently available for SPAAC but displaying unprecedented levels of reactivity should be possible.

Alkynyl crown ethers, recently used in Diels–Alder reactions for the synthesis of supramolecular ion binding crownphanes,<sup>34</sup> provide an accessible platform for click reactions accelerated via transition-state stabilization. The propargylic C–O bonds are stereoelectronically aligned acceptors that can be activated by metal coordination (Figure 2). The proper alignment of acceptors in the starting alkynyl crown ether eliminates part of the entropic penalty their linear analogues must pay to reach the TS and here we show that alkynyl crown ethers, do indeed, react faster. Additionally, we wanted to investigate the possibility of rate acceleration of cycloaddition through coordination of potassium ion, which can potentially be a new approach for TS stabilization through ion sensing.

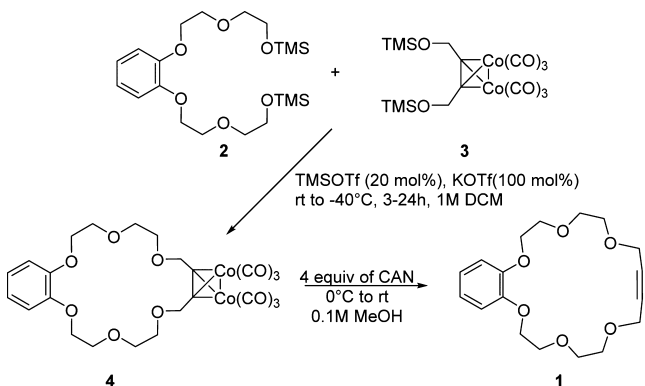
## RESULTS

We set out first to test our predictions of transition-state stabilization provided by antiperiplanar  $\sigma$ -acceptors at the propargylic position via a combination of experimental and computational studies. Experimental studies include a full kinetic analysis for the cycloaddition of the alkynyl crown ether followed by comparison of its reactivity with other alkynes through competition experiments. The computational analysis

involved calculation of cycloaddition barriers with the inclusion of solvation effects followed by the natural bond orbital analysis of TS stabilizing effects responsible for the observed difference in reactivities.

The macrocyclic alkynyl crown ether **1** was synthesized by the dynamic covalent chemistry (DCC)<sup>35</sup> approach based on the Nicholas ether-exchange reaction, as described previously (Scheme 1).<sup>34a</sup> In particular, a mixture of disilyl ether **2** and

**Scheme 1. Synthesis of Alkynyl Crown Ether 4**



alkyne complex **3** was treated with a catalytic amount of TMSOTf in the presence of KOTf as a template of crown ether, and then the cobalt carbonyl moiety was deprotected by CAN to obtain alkyne **1**.<sup>34a</sup>

**Kinetic Analysis.** Rates of cycloaddition with benzyl azide were obtained for the alkynyl crown ether both in the presence (**1-K<sup>+</sup>**) and absence (**1**) of potassium triflate, using <sup>1</sup>H NMR analysis with benzyl phenyl ether as an internal standard. Activation parameters for the crown ether in the presence of potassium triflate were obtained from Arrhenius and Eyring plots (Figure 3).

The energy of activation was found to be 17.7 kcal/mol, while the enthalpy of activation was slightly lower at 17.0 kcal/mol. When entropy is taken into account, the free energy of activation was found to be 21.8 kcal/mol at 25 °C.<sup>36</sup>

The observed rate upon potassium coordination was twice as large as that of the “uncatalyzed” reaction (Figure 4). This rate increase suggests that ion sensing via increased transition-state stabilization is possible. Although ion coordination does not

provide dramatic rate acceleration, alternative alkynyl crown ethers can be designed that take advantage of larger geometric changes upon ion binding. The smaller sodium ion was investigated in attempts to provide more strain in the starting alkyne; however, the rate enhancements were not as dramatic as in the case of potassium coordination ( $1.0 \times 10^{-4}$  vs  $1.3 \times 10^{-4} \text{ M}^{-1} \text{ s}^{-1}$ , see the Supporting Information).

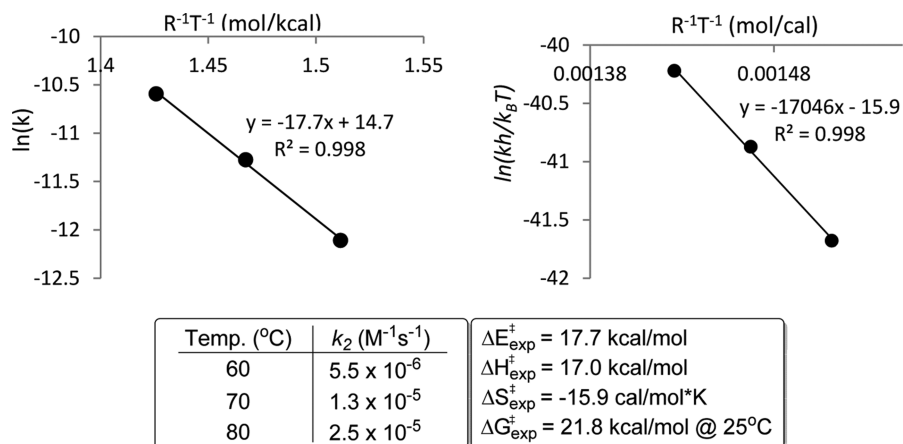
**Relative Kinetics.** In order to compare the reactivity of alkyne **1** versus that of linear alkynes **5–8**, a solution of two alkynes and benzyl azide (0.5 M CD<sub>3</sub>CN, with and without KOTf) was heated to 80 °C for 24 h as shown in Figure 5. The crown ether alkyne was thus compared with a linear analogue (**5**, bearing two propargylic methoxyethoxyethyl ethers) as well as three other linear alkynes bearing 0, 1, or 2 propargylic ether substituents (**6–8**). The ratio of triazole products (**1a**: **5a–8a**) was determined by <sup>1</sup>H NMR.

The results of the competition experiments are given in Figure 5. In all cases, the crown ether was the most reactive alkyne. Furthermore, the presence of potassium ions increased the crown ether reactivity by the factor of 2 relative to all four alkynes (**5–8**). Note that the presence of propargylic oxygen atoms led to significant acceleration relative to the simple dialkyl-substituted alkyne. One propargylic C–O bond led to >12-fold increase in reactivity. Introduction of the second C–O moiety led to a smaller but still significant (~3-fold) reactivity increase. These reactivity trends fully support the hyperconjugative assistance model suggested in our early work.<sup>26,32</sup>

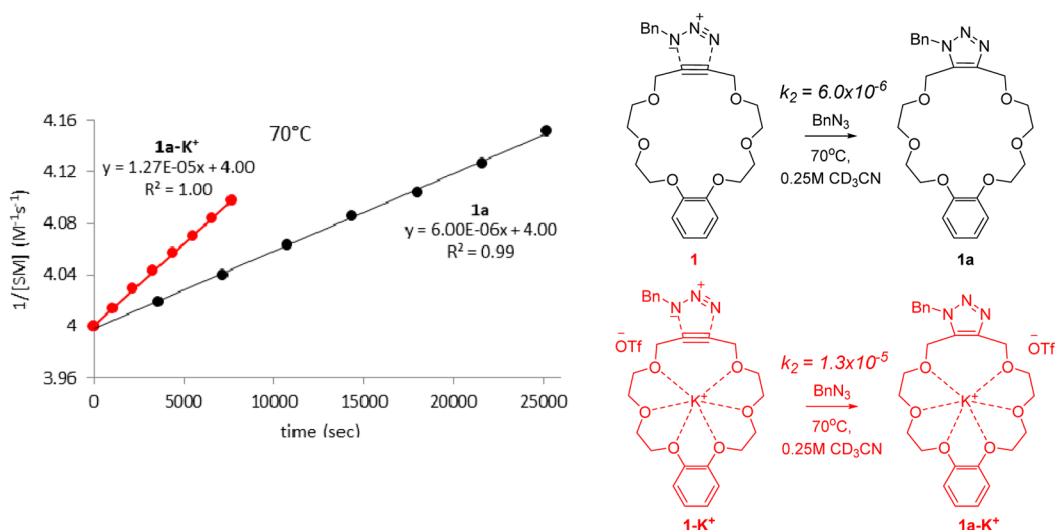
As **1** and **1-K<sup>+</sup>** are predicted to be nearly linear (see the Computational Details), there must be another factor leading to faster reaction kinetics relative to linear analogues which are able to utilize both hyperconjugative stabilization and H-bonding simultaneously. The crown ether scaffold preorganizes the alkyne and propargylic C–O bonds into the geometry required to maximize hyperconjugative stabilization, potentially decreasing the entropic penalty required in order to reach the TS.

## ■ COMPUTATIONAL DETAILS

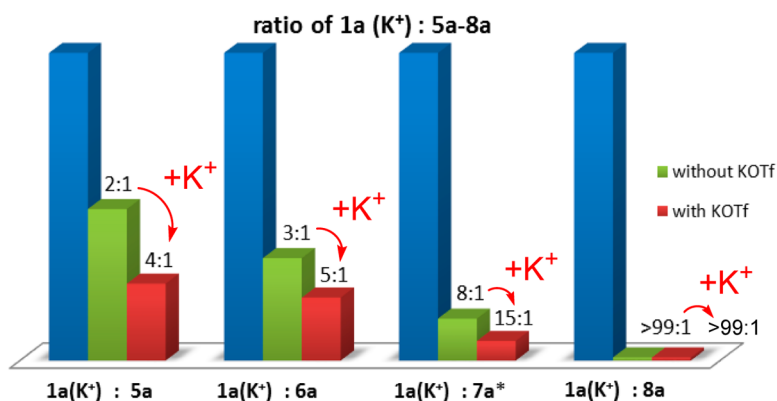
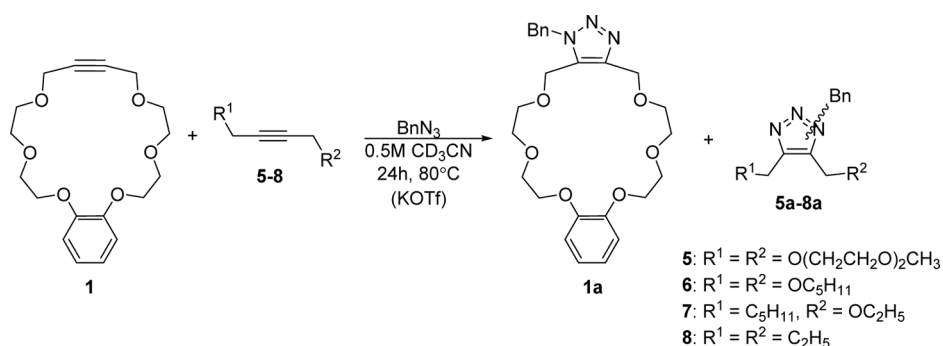
The computational analysis of potential energy profiles for azide–alkyne cycloadditions was performed at the B3LYP/6-31G(d) and M06-2X/6-31G(d) levels of theory using Gaussian 09.<sup>37</sup> For 1,3-dipolar cycloadditions, B3LYP/6-31G(d) and B3LYP/6-31+G(d,p) have mean absolute deviations of 1.5 and 2.6 kcal/mol, respectively, relative to the highly accurate multicomponent CBS-QB3 method for



**Figure 3.** Arrhenius (left) and Eyring (right) plots for the conversion of alkyne **1-K<sup>+</sup>** into triazole **1a-K<sup>+</sup>**. The determined rates at each temperature and the activation parameters are given below.



**Figure 4.** Rate constants ( $\text{M}^{-1} \text{s}^{-1}$ ) determined by monitoring product formation relative to an internal standard at  $70^\circ\text{C}$  for the cycloaddition of alkyne crown ether accelerated by potassium ion coordination.



**Figure 5.** Competition experiments with the alkyne crown ether **1** and **1-K<sup>+</sup>** and various alkynes **5–8** at  $0.5 \text{ M CD}_3\text{CN}$ ,  $80^\circ\text{C}$ . Product ratios are given in the presence (red) and absence (green) of KOTf relative to **1a** (blue). \*Regioisomers were obtained in a  $\sim 1:1$  ratio.

activation barriers.<sup>38</sup> It has been reported, however, that B3LYP does not describe noncovalent interactions as accurately as M06-2X.<sup>39</sup>

Frequency calculations were performed to confirm each stationary point as minima or first-order saddle points. Solvation corrections were performed on the gas-phase geometries. A CPCM dielectric continuum solvent model for acetonitrile with both UA0 and UFF radii was employed. This model does not explicitly include nonelectrostatic contributions, cavitation, and dispersion energies and should be considered as the first approximation of solvation effects.<sup>40</sup> UA0 radii were used previously by Houk and co-workers for related cycloadditions.<sup>25b</sup>

Electronic structures of reactants and transition states were analyzed using natural bond orbital (NBO) analysis. The NBO 4.0<sup>41</sup> program was used to evaluate the energies of hyperconjugative interactions. The

NBO analysis transforms the canonical delocalized Hartree–Fock (HF) MOs or corresponding natural orbitals of alternate descriptions (i.e., DFT) into localized orbitals that are closely tied to chemical bonding concepts. Filled NBOs describe the hypothetical localized Lewis structure. The interactions between filled and vacant orbitals represent the deviation of the molecule from the Lewis structure and can be used as a measure of delocalization.<sup>23i,42</sup> This method gives energies of hyperconjugative interactions both by deletion of the off-diagonal Fock matrix elements between the interacting orbitals and from the second-order perturbation approach

$$E(2) = -n_{\sigma} \frac{\langle \sigma F / \sigma^* \rangle^2}{\epsilon_{\sigma^*} - \epsilon_{\sigma}} = -n_{\sigma} \frac{F_{ij}^2}{\Delta E} \quad (1)$$



where  $\langle \sigma/F/\sigma^* \rangle$  or  $F_{ij}$  is the Fock matrix element between the  $i$  and  $j$  NBO orbitals,  $\epsilon_\sigma$  and  $\epsilon_{\sigma^*}$  are the energies of  $\sigma$  and  $\sigma^*$  NBO's, and  $n_\sigma$  is the population of the donor  $\sigma$  orbital.<sup>43,44</sup> From the NBO analysis, overlap integrals were obtained from the preorthogonalized NBOs. Detailed descriptions of the NBO calculations are available in the literature.<sup>45,46</sup>

## COMPUTATIONAL RESULTS

**Reactivity of Crown Ethers.** The activation energies calculated at M06-2X/6-31G(d) for **1** and **1-K<sup>+</sup>** were 13.4 and 12.8 kcal/mol, respectively. At the B3LYP/6-31G(d), the barriers for **1** and **1-K<sup>+</sup>** were predicted to be slightly higher (18.7 and 15.4 kcal/mol, respectively). The modest rate increase upon potassium ion coordination ( $\sim 2\times$ ) determined experimentally follows more closely with the difference in activation barriers predicted at the M06-2X/6-31G(d) level of theory (0.6 kcal/mol). On the other hand, the absolute value of the experimental activation energy obtained from the Arrhenius analysis for **1-K<sup>+</sup>** (17.7 kcal/mol, Figure 7) matches more closely the B3LYP/6-31G(d) value (15.4 kcal/mol). Both computational methods underestimate the experimentally obtained barrier. These differences are discussed below.

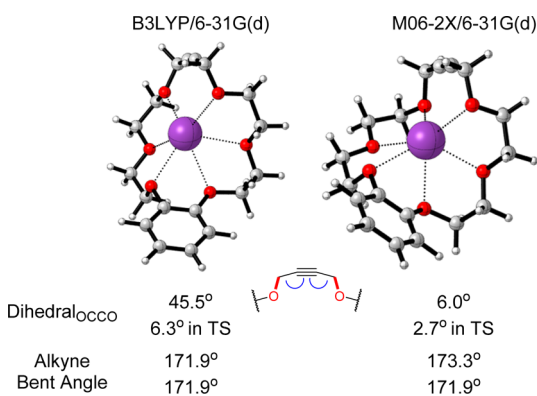
The different levels of theory predict slightly different conformations for the potassium-coordinated SM **1-K<sup>+</sup>**, leading to the varying degrees of hyperconjugative assistance in the TS (Table 1, below) and

**Table 1.** NBO Analysis of Increasing Hyperconjugative Assistance to the Cycloaddition Transition State between the in-Plane Alkyne  $\pi$ -System and (Sum of) Two Propargylic  $\sigma^*_{C-O}$  Acceptors in Alkynyl Crown Ether upon Ion Coordination<sup>a</sup>

$\pi + \pi^* \rightarrow \sigma^*_{CO}$ (kcal/mol)	starting alkyne M062X(B3LYP)/ 6-31G(d)	transition state M062X(B3LYP)/ 6-31G(d)	hyperconjugative assistance <sup>b</sup> M062X(B3LYP)/ 6-31G(d)
<b>1</b>	13.6 (12.6)	19.1 (17.5)	5.5 (4.9)
<b>1-K<sup>+</sup></b>	12.7 (10.2)	21.5 (21.4)	8.8 (11.2)

<sup>a</sup>Values given for gas phase. <sup>b</sup>Hyperconjugative assistance defined as difference in interaction energies between the reacting  $\pi$ -bond and the hyperconjugative acceptor ( $\pi + \pi^* \rightarrow \sigma^*_{CO}$ ) between the TS and SM.

thus different effects on the cycloaddition barrier (Figure 6). At the B3LYP/6-31G(d) level, the OCCO dihedral angle (red bonds, Figure 6) is 45.5° in the starting alkyne and 6.3° in the TS. At the M06-2X/6-31G(d) level, the OCCO dihedral angle changes from 6.0° in the



**Figure 6.** Geometries of the lowest energy alkynyl crown ether-potassium complex **1-K<sup>+</sup>** optimized at the B3LYP/6-31G(d) and M062X/6-31G(d) levels of theory. Dihedral angles given for the OCCO bonds in red. The degree of bending in the alkyne is given as the bent angle (blue).

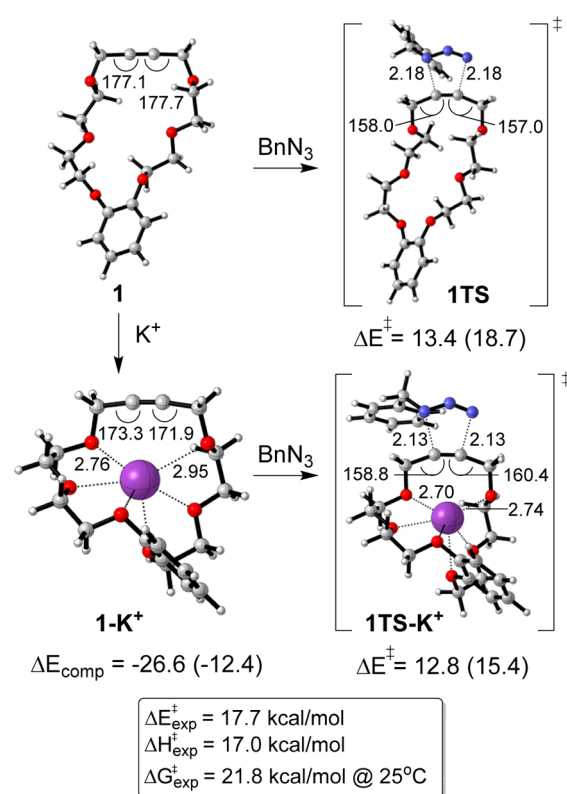
starting alkyne to 2.7° in the TS. In the gas phase, the “aligned” conformation was predicted to be 0.4 kcal/mol less stable at the B3LYP level of theory, but 0.7 kcal/mol more stable at M06-2X.

The optimized structures of the free alkynyl crown ether **1** and its potassium complex **1-K<sup>+</sup>** and transition states for the cycloadditions with benzyl azide are shown in Figure 7. The alkyne moiety in the free crown ether is essentially linear, with the CCC angles of  $\sim 177$ – $178^\circ$ . Although potassium coordination introduces some bending, the deviation from linearity is small (CCC angles of  $172$ – $173^\circ$ ).<sup>47</sup> On the basis of previous calculations,<sup>26</sup> bending to  $170^\circ$  corresponds to a 2.0 kcal/mol energy penalty for 2-butyne. Incorporation of one antiperiplanar C–F acceptor in 1-fluoro-2-butyne reduces this penalty to 1.8 kcal/mol, while in **1** and **1-K<sup>+</sup>** two antiperiplanar C–O acceptors are present to alleviate the energy cost for alkyne bending.<sup>32</sup>

These small deviations from linearity suggest that most of the increased reactivity of alkynyl crown ethers should be due to TS stabilization (through hyperconjugative assistance) rather than destabilization of the reactant. This observation suggests alkynyl crown ethers should benefit from TS stabilization in two different ways, as was previously suggested for unstrained systems:<sup>26</sup> (a) a decreased energy cost for alkyne bending and (b) assistance to bond formation.

The energy of ion complexation differed greatly from  $-26.6$  kcal/mol at M06-2X/6-31G(d) to  $-12.4$  kcal/mol for B3LYP/6-31G(d) (Figure 7). This result is likely to stem from the inadequacy of B3LYP in describing noncovalent interactions.<sup>39</sup>

Other than the expected geometrical change of increased alkyne bending in the TS, the only other major difference was the shortened propargylic oxygen-potassium distance ( $\sim 0.2$  and  $0.06$  Å), with much



**Figure 7.** Geometries of starting alkynyl crown ether and crown ether-potassium complex optimized at the M06-2X/6-31G(d) level of theory with angles given in degrees and propargylic O–K<sup>+</sup> bond lengths given in angstroms. Energies of activation and complexation given in kcal/mol for CPCM (acetonitrile, radii = UA0) solvation corrections (single point on gas phase geometries), with B3LYP/6-31G(d) values given in parentheses. Experimental activation parameters for the potassium “catalyzed” reaction **1-K<sup>+</sup>**.

smaller variations in other O–K<sup>+</sup> distances. The total energy of n<sub>O</sub> → K<sup>+</sup> interactions provided by NBO analysis increase from 71.2 kcal/mol in the starting alkyne to 72.9 kcal/mol in the TS. This tighter binding in the TS suggests the possibility of a new strategy for selective TS stabilization, which may provide a new platform for the development of stable, yet reactive alkynes that can be activated on demand. There are also small variations in the *gauche* OCCO geometry in each moiety of the crown ether, with the largest change being the movement closer toward the ideal 60° angle (from 57.7° to 58.9°).

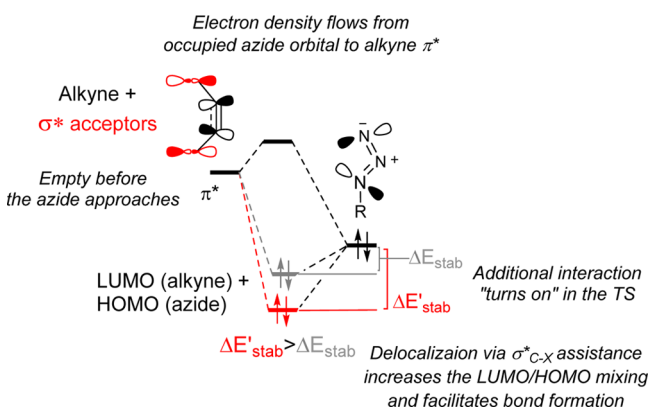
NBO analysis suggests that potassium ion coordination provides additional hyperconjugative assistance in the TS (Table 1, NBO analysis) and thus lowers the barrier. The difference in activation energies between **1** and **1–K<sup>+</sup>** is much smaller at M06-2X/6-31G(d) (0.6 kcal/mol) than at B3LYP/6-31G(d) (3.3 kcal/mol), which is reflected by the smaller magnitude of calculated hyperconjugative assistance.

Both levels of theory suggest the potassium ion makes the propargylic CO bonds better acceptors in the TS, providing for the larger overall assistance (Table 1). The larger magnitude of hyperconjugative assistance predicted at the B3LYP/6-31G(d) level of theory most likely stems from the larger difference in OCCO dihedral angles between the starting alkyne and TS in **1–K<sup>+</sup>** (from 45.5° to 63°) relative to the geometries predicted at the M06-2X/6-31G(d) level (6.0° to 2.7°, Figure 6).

It is somewhat puzzling that the sum of  $\pi \rightarrow \sigma^*_{CO}$  interactions decreases in the starting alkyne when potassium is coordinated. NBO analysis of the M06-2X/6-31G(d) optimized structures suggests there is a very slight decrease in  $\pi / \sigma^*_{CO}$  overlap upon potassium ion coordination, which is reflected in the  $F_{ij}$  term (eq 1, see the Supporting Information for details). This decrease in overlap upon ion binding seems to stem from alkyne bending, as the OCCO dihedral angle only changes ~0.5°.

The relatively small change in dihedral angles in the TS relative to the starting geometry for **1–K<sup>+</sup>** predicted at M06-2X/6-31G(d) suggests the increased interaction energy is not largely due to increased orbital overlap during cycloaddition, but either a decreased energy gap between interacting orbitals or increased electron population in the donor orbital (eq 1). Increase in the donor orbital population is the major factor, as orbital interactions in the transition state redirect electron density from the azide to the alkyne  $\pi^*$ . Propargylic acceptors provide the opportunity for an additional  $\pi^* \rightarrow \sigma^*$  interaction that is absent in the starting alkyne, providing greater stabilization and, in turn, assisting in bond formation (Figure 8).<sup>26,32</sup>

This charge transfer from the azide into the alkyne  $\pi^*$ , facilitated by delocalization into propargylic acceptor bonds, is strengthened when the potassium ion is present. Delocalization occurs both via increased



**Figure 8.** Key aspect of selective TS stabilization in alkynes utilizing hyperconjugative interactions for increased reactivity.<sup>48</sup> Assistance to C–N bond formation is provided by an increased interaction when propargylic acceptors are present (red). The lower stabilization provided by such an interaction when  $\sigma$ -acceptors are absent is shown in gray.

hyperconjugative interactions (~9–11 kcal/mol) as well as via through space interactions between the oxygen lone pairs and the potassium ion (see above, ~1.7 kcal/mol), the alkyne  $\pi$  system and the potassium ion (<0.1 kcal/mol), and surprisingly, directly between the azide and potassium ion (<1.0 kcal/mol total).<sup>49</sup> However, NBO analysis suggests these through-space interactions are small, with increased hyperconjugative interactions as the major contributor. The appearance of this additional interaction that is absent in the starting materials is key for selective TS stabilization.

Similar conclusions can be made from the distortion analysis, a method for dissection of transition-state effects developed by Houk and co-workers.<sup>25a,b,29</sup> The crown alkynes have lower distortion energies than acyclic alkynes listed in Table 2.<sup>50</sup> Furthermore, the interaction energies between the alkyne and azide for the crown reagent **1–K<sup>+</sup>** is the largest, and **1** is only surpassed by **7'** (however, **7'** has a much higher distortion energy for both the alkyne and azide relative to **1**). Both effects (the low distortion penalty and favorable increase in the attractive interactions) decrease the cycloaddition barrier. As usual in such cycloadditions, however, the bulk of distortion energy comes from the distortion of the second reagent (azide). The increased magnitude of this contribution partially offsets the two accelerating effects.

**Reactivity of Acyclic Alkynes.** Barriers for the cycloadditions of benzyl azide with various alkynes bearing substituents similar to those used in our competition studies (Figure 5) calculated at the M06-2X/6-31G(d) level of theory are given in Figure 9 (for B3LYP/6-31G(d) values, see the Supporting Information). The trend in relative reactivity of crown alkynes and linear analogues predicted at the M06-2X/6-31G(d) level of theory (CPCM = MeCN, radii = UA0) are consistent with the reactivity observed in competition studies (Figure 5). The barrier for the 1,4-dimethoxy-2-butyne **6'** is predicted to be lower than that of crown ether **1** without potassium coordination in the gas phase (11.2 vs 11.5 kcal/mol, respectively), due to the potential for H-bonding interactions in **6'**. While solvation corrections (CPCM = MeCN) alleviate this discrepancy, the barrier for **1** is comparable to **1–K<sup>+</sup>** with radii = UFF (13.4 vs 13.3 kcal/mol, respectively). The  $\Delta\Delta E^\ddagger$  between **1** and **1–K<sup>+</sup>** of 0.6 kcal/mol with radii = UA0 matches more closely the ~2× rate increase determined experimentally (Figure 4) and the nearly 2-fold increase in selectivity upon addition of potassium triflate in relative kinetics studies (Figure 9).

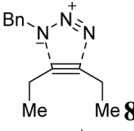

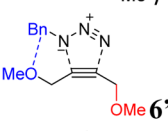
Surprisingly, at the B3LYP/6-31G(d) level of theory, the barrier for 1,4-dimethoxy-2-butyne **6'** is predicted to be lower than the barrier for the crown **1**, even with solvation corrections included (see the Supporting Information). This may stem from the inadequate solvation approximation methods. The preferred gas-phase geometry of **1** was less stable than an alternate conformation when solvation corrections are included (see the Supporting Information for geometries and relative energies).

The barrier decrease of **1** and **1–K<sup>+</sup>** relative to **6'** suggests that the slight deviation from the linear geometry (Figure 7) may provide some rate enhancement via strain activation; however, the crown alkyne is also preorganized to resemble the transition-state geometry, decreasing the entropic penalty to reach the TS. Compound **6'** is predicted to benefit from both of the previously identified<sup>26</sup> TS stabilizing effects: (a) hyperconjugative assistance from the antiperiplanar  $\sigma^*_{CO}$  and (b) the electrostatic H-bonding interaction between the azide substituent (Bn) and the oxygen lone pair. This TS was preferred over the conformation in which both propargylic C–O bonds are antiperiplanar both in the gas phase and with the inclusion of solvation corrections. Both TS stabilizing effects are possible in the nonsymmetric ether **7'**, although not simultaneously. The lack of available cooperative effects leads to slower reactivity, which is apparent from the competition studies (Figure 5).

## CONCLUSIONS

Alkynyl crown ethers have provided experimental verification of our predictions that noncatalyzed azide/alkyne cycloadditions can be accelerated via transition-state stabilization. The alkynyl

Table 2. Activation, Distortion, and Interaction Energies for the Cycloadditions of Benzyl Azide with Various Alkynes Calculated at the M06-2X/6-31G(d) Level of Theory

	$\Delta E^\ddagger$ , kcal/mol	$E_{\text{Dist}}$ Alkyne, kcal/mol	$E_{\text{Dist}}$ Azide, kcal/mol	$E_{\text{Dist}}$ Total, kcal/mol	$E_{\text{Int}}$ , kcal/mol
	Gas phase MeCN <sup>a,b</sup>	Gas phase MeCN <sup>a,b</sup>	Gas phase MeCN <sup>a,b</sup>	Gas phase MeCN <sup>a,b</sup>	Gas phase MeCN <sup>a,b</sup>
	15.7 17.0	8.8 8.7	19.4 19.6	28.2 28.3	-12.5 -11.3
	13.7 15.4	9.7 9.6	18.6 18.8	28.4 28.4	-15.3 -13.1
	11.2 13.8	9.8 10.1	17.8 17.9	27.7 27.9	-13.1 -14.1
<b>1</b>	11.5 13.4	7.4 8.1	17.4 17.6	24.9 25.6	-13.3 -12.3
<b>1-K<sup>+</sup></b>	9.4 12.8	7.6 7.1	20.6 20.4	28.3 27.5	-18.9 -14.7
Cyclooctyne	7.5 8.7	2.4 2.3	15.9 16.1	18.3 18.3	-10.8 -9.6

<sup>a</sup>Gas-phase geometry. <sup>b</sup>CPCM (dielectric continuum solvent model), radii = UA0.

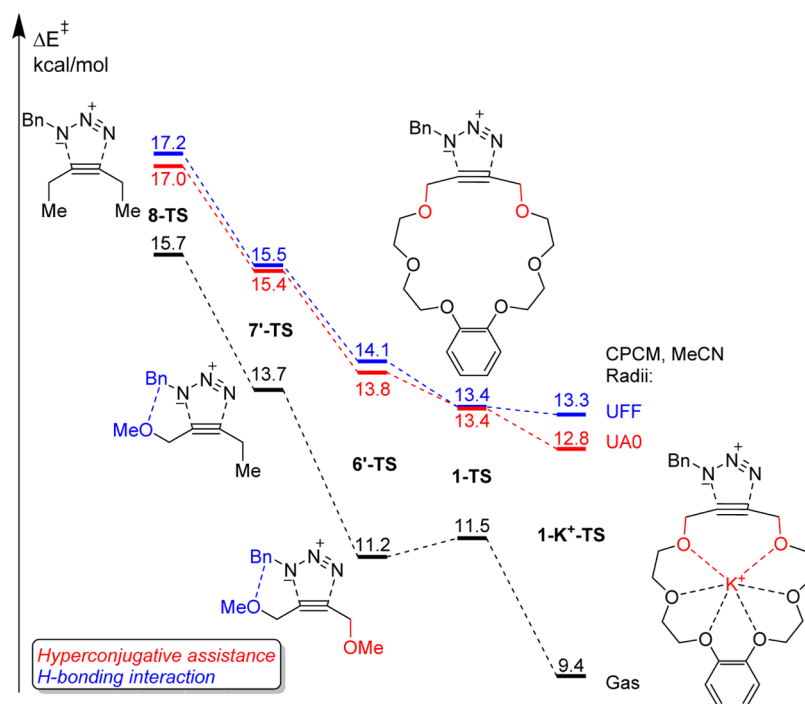


Figure 9. Activation barriers for the cycloadditions of benzyl azide with various alkynes calculated at the M06-2X/6-31G(d) level of theory with CPCM (acetonitrile, radii are color coded) solvation corrections (single point on gas phase geometries). Lowest energy TSs are shown.

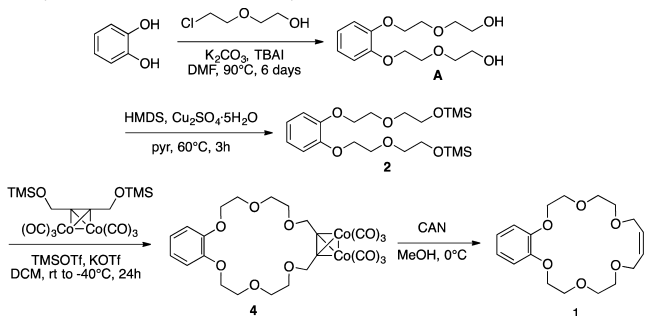
crown ethers react faster than both alkyl-substituted alkynes and their linear analogues. While linear dipropargyl ethers can benefit from two stabilizing effects simultaneously (hyperconjugative assistance and C–H...O H-bonding interactions), the crown ether moiety preorganizes the propargylic acceptors into the optimal orbital arrangement to provide stereoelectronic stabilization to the transition state. Such preorganization decreases the entropic penalty to reach the TS geometry.

A 2-fold rate enhancement was observed upon potassium ion coordination. While the rate acceleration through ion-coordination of potassium ion is not dramatic, the optimization of this effect shows promise for use in ion sensing by way of a new type of metal-catalyzed click reaction. Currently, the preparation of smaller cycloalkynes that can take advantage of both TS stabilization and strain activation is underway.

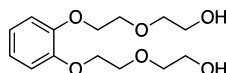
## EXPERIMENTAL SECTION

**1. General Information.**  $^1\text{H}$  and  $^{13}\text{C}$  NMR spectra were recorded on a 400 MHz spectrometer using  $\text{CDCl}_3$  and  $\text{CD}_3\text{CN}$  as the deuterated solvents. The chemical shifts ( $\delta$ ) are reported in parts per million (ppm) relative to the residual  $\text{CHCl}_3$  peak (7.26 ppm for  $^1\text{H}$  NMR and 77.0 ppm for  $^{13}\text{C}$  NMR) and  $\text{CD}_3\text{CN}$  (1.96 ppm for  $^1\text{H}$  NMR and 1.32 ppm for  $^{13}\text{C}$  NMR). The coupling constants ( $J$ ) are reported in hertz (Hz). IR spectra were recorded on a FT-IR spectrometer with diamond ATR accessory as thin film. Mass spectra were recorded using electrospray ionization (ESI) or electron impact (EI). Yields refer to isolated material judged to be  $\geq 95\%$  pure by  $^1\text{H}$  NMR spectroscopy following silica gel chromatography. All the chemicals were used as received unless otherwise stated. All solvents, solutions, and liquid reagents were added via syringe. Tetrahydrofuran (THF) and methylene chloride ( $\text{CH}_2\text{Cl}_2$ ) were dried over a column of molecular sieves under nitrogen. The *n*-BuLi solutions were titrated against a known amount menthol dissolved in tetrahydrofuran using 1,10-phenanthroline as the indicator. All reactions were carried out under an inert nitrogen atmosphere unless otherwise stated. The purifications were performed by flash chromatography using silica gel F-254 (230–499 mesh particle size).

### Synthesis of Starting Alkyne 1.



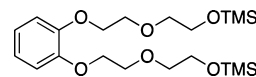
### 2,2'-((1,2-Phenylenebis(oxy))bis(ethane-2,1-diyl))bis(oxy))bis(ethan-1-ol) (A).



To a reaction mixture of pyrocatechol (4.00 g, 36.3 mmol), potassium carbonate (50.2 g, 363 mmol), and potassium iodide (15.1 g, 91 mmol) in dried DMF (121 mL, 0.3 M) was added 2-(2-chloroethoxy)ethanol (15.3 mL, 145 mmol). The reaction mixture was heated at 90 °C for 3 days. After that, the mixture was cooled, diluted with water, and extracted with chloroform (3 $\times$ ). The combined organic was washed with brine, dried over magnesium sulfate, and then concentrated under vacuo. The crude product was purified by flash chromatography on silica gel (5% MeOH/ $\text{CHCl}_3$ ) to afford 6.02 g (58% yield) of 2,2'-((1,2-phenylenebis(oxy))bis(ethane-2,1-diyl))bis(oxy))bis(ethan-1-ol) (A) as a colorless oil. The spectroscopy data were matched to the known compound:  $^1\text{H}$  NMR (400

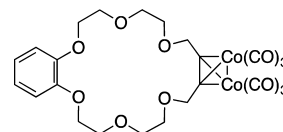
MHz)  $\delta$  3.65–3.69 (m, 4H), 3.70–3.78 (m, 6H), 3.88–3.90 (m, 4H), 4.14–4.16 (m, 4H), 6.87–6.92 (m, 4H);  $^{13}\text{C}$  NMR (100 MHz)  $\delta$  61.6, 68.3, 69.3, 72.8, 113.5, 121.5, 148.4.

### 1,2-Bis(2-(2-((trimethylsilyl)oxy)ethoxy)ethoxy)benzene (2).



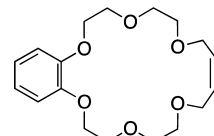
To a solution of 1,2-bis[2-(2-hydroxyethoxy)ethoxy]benzene (3.38 g, 11.8 mmol) in pyridine (11.8 mL) were added hexamethyldisilazane (16.6 mL, 79 mmol) and copper(II) sulfate pentahydrate (0.442 g, 1.77 mmol), and the reaction mixture was allowed to stand at 60 °C for 18 h. After addition of 5% copper(II) sulfate solution, the product was extracted by ethyl acetate. The combined organic layer was washed with brine, dried over sodium sulfate, and concentrated to obtain a yellow oil. The crude product was purified by flash chromatography on silica gel (1% to 5% MeOH/ $\text{CHCl}_3$ ) to afford 1,2-bis(2-(2-((trimethylsilyl)oxy)ethoxy)ethoxy)benzene (2) (4.58 g, 90% yield) as a colorless oil. The spectroscopy data was matched to the known compound:  $^1\text{H}$  NMR (400 MHz)  $\delta$  0.12 (s, 18H), 3.64 (t,  $J$  = 4.9 Hz, 4H), 3.75 (t,  $J$  = 4.9 Hz, 4H), 3.85 (t,  $J$  = 4.9 Hz, 4H), 4.16 (t,  $J$  = 4.9 Hz, 4H), 6.89–6.95 (m, 4H);  $^{13}\text{C}$  NMR (100 MHz)  $\delta$  62.0, 68.8, 69.8, 72.8, 115.0, 121.6, 149.0.

### Cobalt Complex (4).



In a dried flask was placed potassium trifluoromethanesulfonate (93.0 mg, 2.00 mmol) under nitrogen atmosphere. A solution of cobalt complex 3 (1.04 g, 1.99 mmol) and disilyl ether 2 (0.87 g, 2.03 mmol) in dichloromethane (2.0 mL, 1 M) was added, and then trimethylsilyl trifluoromethanesulfonate (75  $\mu\text{L}$ , 0.42 mmol) was added dropwise via syringe at room temperature. The reaction mixture was stirred at the same temperature for 3 h, followed by stirring at  $-40$  °C for 24 h. Solid sodium hydrogen carbonate was added before the insoluble solid was filtered off, and the filtrate was evaporated in vacuo. The residual red oil was purified by flash chromatography on silica gel (15%  $\rightarrow$  30%  $\rightarrow$  100% ethyl acetate/hexanes) to afford cobalt complex crown ether 4 (0.85 g (68% yield)). The spectroscopy data were matched to the known compound:  $^1\text{H}$  NMR (400 MHz)  $\delta$  3.83–3.87 (m, 8H), 3.91 (t,  $J$  = 4.3 Hz, 4H), 4.15 (t,  $J$  = 4.3 Hz, 4H), 4.77 (s, 4H), 6.86–6.92 (m, 4H);  $^{13}\text{C}$  NMR (100 MHz)  $\delta$  58.3, 68.3, 68.7, 69.2, 70.3, 82.7, 113.8, 121.2, 148.7.

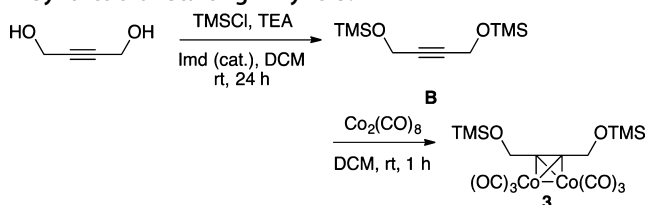
### Alkynyl Crown Ether (1).



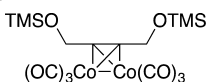
To a solution of cobalt complex crown ether 4 (3.5 g, 5.6 mmol) in methanol (56 mL, 0.1 M) was slowly added a solution of cerium(IV) diammonium nitrate (12.4 g, 22.6 mmol) in methanol at 0 °C. The reaction mixture was diluted with water and extracted with chloroform (3 $\times$ x). The organic layer was dried over sodium sulfate and concentrated in vacuo. The crude product was purified by flash chromatography on silica gel (5% to 10% MeOH/ $\text{CHCl}_3$ ) to afford crown ether 1 (1.4 g (75% yield)) as solid. The spectroscopy data were matched to the known compound: mp (MeOH/ $\text{CHCl}_3$ ) 78–79 °C; IR (neat)  $\nu_{\text{max}}$  2920, 2688, 1592, 1505, 1453, 1349, 1255, 1220, 1126, 1101, 1054  $\text{cm}^{-1}$ ;  $^1\text{H}$  NMR (400 MHz)  $\delta$  3.76–3.82 (m, 8H), 3.89 (t,  $J$  = 4.5 Hz, 4H), 4.15 (t,  $J$  = 4.8 Hz, 4H), 4.22 (s, 4H), 6.84–6.90 (m, 4H);  $^{13}\text{C}$  NMR (100 MHz)  $\delta$  58.3, 68.3, 68.7, 69.2, 70.3, 82.7, 113.8, 121.2, 148.7; HRMS (ESI $^+$ , TOF) calcd for  $\text{C}_{18}\text{H}_{24}\text{O}_6\text{Na}$  ( $M + \text{Na}^+$ ) 359.1471, found 359.1467.



## Synthesis of Starting Alkyne 3.

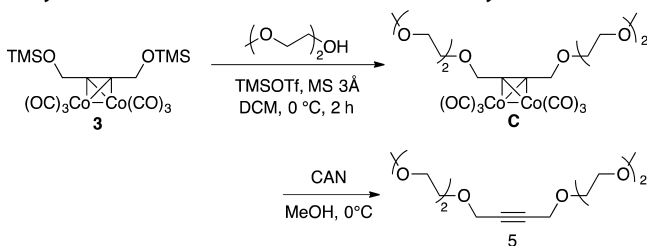
2,2,9,9-Tetramethyl-3,8-dioxa-2,9-disiladec-5-yne (B).<sup>34</sup>

To solution of but-2-yne-1,4-diol (1.0 g, 11.6 mmol) in DCM (23 mL, 0.5 M) were added imidazole (158 mg, 2.3 mmol) as catalyst and triethylamine (4.9 mL, 34.8 mmol) at 0 °C. The reaction mixture was stirred for 10 min, and then TMSCl (3.1 mL, 24.4 mmol) was added dropwise. The reaction mixture was warmed to room temperature for 18 h and then was concentrated to give crude oil. The crude product was purified by flash chromatography on silica gel (hexanes to 5% EtOAc/hexanes) to afford 2,2,9,9-tetramethyl-3,8-dioxa-2,9-disiladec-5-yne (B) (1.7 g, 64% yield) as a colorless liquid. The spectroscopy data was matched to the known compound:  $^1\text{H}$  NMR (400 MHz)  $\delta$  -0.16 (s, 18H), 4.31 (s, 4H);  $^{13}\text{C}$  NMR (100 MHz)  $\delta$  -0.40, 51.1, 82.4.

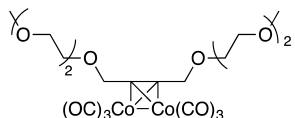
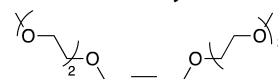
Cobalt Complex 3.<sup>52</sup>

To solution of 1,4-bis(trimethylsilyloxy)but-2-yne B (1.5 g, 6.5 mmol) in DCM (26 mL, 0.25 M) was added dicobalt octacarbonyl (2.3 g, 2.8 mmol) at room temperature. The reaction was stirred for 1 h, and then the mixture was concentrated to give crude red oil. The crude product was purified by flash chromatography on silica gel (hexanes to 5% EtOAc/hexanes) to afford cobalt complex 3 3.4 g (96% yield) as red oil. The spectroscopy data was matched to known compound:  $^1\text{H}$  NMR (400 MHz)  $\delta$  -0.16 (s, 18H), 4.76 (s, 4H);  $^{13}\text{C}$  NMR (100 MHz)  $\delta$  -0.74, 62.8, 96.0.

## Synthesis of 2,5,8,13,14,17-Hexaoxaicos-10-yne (5).

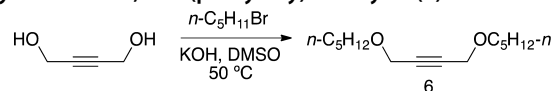


**Cobalt Complex C.**<sup>34</sup> In a dried flask were placed molecular sieves 3A (0.426 g) under nitrogen atmosphere. The solution of cobalt complex 3 (1.0 g, 2.09 mmol) and 2-(2-methoxyethoxy)ethanol (0.5 mL, 4.26 mmol) in dichloromethane (4.20 mL, 0.5 M) were added, and then trimethylsilyl trifluoromethanesulfonate (0.19 mL, 1.04 mmol) was added dropwise via syringe at 0 °C. The reaction mixture was stirred at the same temperature for 2 h. After that, the reaction was quenched with saturated sodium bicarbonate solution at the same temperature and extracted with DCM (3 $\times$ ). The combined organic was washed with brine, dried over sodium sulfate, and then concentrated under vacuo. The crude red oil was purified by flash chromatography on silica gel (CHCl<sub>3</sub> to 5% MeOH/CHCl<sub>3</sub>) to afford cobalt complex 0.65 g (54% yield) as red oil: IR (neat)  $\nu_{\text{max}}$  2880, 2093, 2051, 2021, 1621, 1455, 1346, 1106 cm<sup>-1</sup>;  $^1\text{H}$  NMR (400 MHz)  $\delta$  3.38 (s, 6H), 3.54 (s, 4H), 3.66 (s, 4H), 3.69 (s, 4H), 3.79 (s, 4H), 4.69 (s, 4H);  $^{13}\text{C}$  NMR (100 MHz)  $\delta$  59.0, 70.5, 70.6, 70.7, 71.4, 71.9, 92.2.

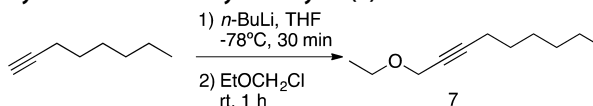
2,5,8,13,14,17-Hexaoxaicos-10-yne (5).<sup>34</sup>

To a solution of cobalt complex C (0.65 g, 1.12 mmol) in methanol (11.0 mL, 0.1 M) was slowly added solution of cerium(IV) diammonium nitrate (2.46 g, 4.49 mmol) in methanol at 0 °C. The reaction mixture was diluted with water and extracted with chloroform (3 $\times$ ). The organic layer was dried over sodium sulfate and concentrated in vacuo. The crude product was purified by flash chromatography on silica gel (5–10% MeOH/CHCl<sub>3</sub>) to afford 2,5,8,13,16,19-hexaoxaicos-10-yne (5) (0.12 g, 36% yield) as a colorless oil: IR (neat):  $\nu_{\text{max}}$  2872, 1456, 1348, 1246, 1199, 1094, 1025 cm<sup>-1</sup>;  $^1\text{H}$  NMR (400 MHz)  $\delta$  3.31 (s, 6H), 3.47–3.49 (m, 4H), 3.55–3.62 (m, 12H) 4.21 (s, 4H);  $^{13}\text{C}$  NMR (100 MHz)  $\delta$  58.9, 69.9, 70.95, 71.01, 72.6, 83.3; HRMS (ESI<sup>+</sup>, TOF) calcd for C<sub>14</sub>H<sub>26</sub>O<sub>6</sub>Na (M + Na<sup>+</sup>) 313.1627, found 313.1626.

## Synthesis of 1,4-Bis(pentyloxy)but-2-yne (6).



To solution of 2-butyne-1,4-diol (1.00 g, 11.6 mmol) in DMSO (11.6 mL, 1 M) were added KOH pellets (1.43 g, 25.6 mmol). The reaction mixture was stirred for 0.5 h, and then 1-bromopentane was added via syringe. The reaction was stirred at 50 °C for 1 h, and then the mixture was poured into ice/water and the product was extracted with ether (3 $\times$ ). The combined organic layer was washed with water and brine and then dried over MgSO<sub>4</sub>. The solution was concentrated to give a crude mixture, which further purified by flash chromatography on silica gel (hexanes to 5% EtOAc/hexanes) to afford 0.93 g (35% yield) of 1,4-bis(pentyloxy)but-2-yne (9) as a colorless oil. The spectroscopy data was matched to known compound:  $^1\text{H}$  NMR (400 MHz)  $\delta$  0.90 (t,  $J$  = 7.0 Hz, 6H), 1.30–1.35 (m, 8H), 1.59 (quint,  $J$  = 7.0 Hz, 4H), 3.49 (t,  $J$  = 6.7 Hz, 4H), 4.17 (s, 4H);  $^{13}\text{C}$  NMR (100 MHz)  $\delta$  13.8, 22.3, 28.1, 29.0, 58.1, 70.1, 82.2.

Synthesis of 1-Ethoxynon-2-yne (7).<sup>53</sup>

To a solution of oct-1-yne (2 mL, 13.6 mmol) in THF (0.5 M, 27 mL) was added  $n\text{-BuLi}$  (10.2 mL, 1.6 M in hexanes) dropwise at -78 °C. The reaction mixture was stirred for 30 min. Then (chloromethoxy)ethane (1.9 mL, 20.3 mmol) was added dropwise and the mixture warmed to room temperature. After 1 h, the reaction mixture was quenched with saturated NH<sub>4</sub>Cl solution followed by extraction with ether (3 $\times$ ). The combined organic layers were washed with brine, dried with MgSO<sub>4</sub>, and then concentrated. The resulting oil was then purified by flash chromatography on silica gel (hexanes to 5% EtOAc/hexanes) to afford 1.65 g (72% yield) of 1-ethoxynon-2-yne 10 as a colorless oil: IR (neat)  $\nu_{\text{max}}$  2931, 2859, 1458, 1351, 1264, 1092, 1011 cm<sup>-1</sup>;  $^1\text{H}$  NMR (400 MHz)  $\delta$  0.88 (t,  $J$  = 6.9 Hz, 3H), 1.22 (t,  $J$  = 7.0 Hz, 3H), 1.24–1.41 (m, 6H), 1.50 (quint,  $J$  = 7.3 Hz, 3H), 2.20 (tt,  $J$  = 7.1, 2.1 Hz, 2H), 3.54 (q,  $J$  = 7.0 Hz, 2H), 4.11 (t,  $J$  = 2.1 Hz, 2H);  $^{13}\text{C}$  NMR (100 MHz)  $\delta$  14.0, 15.0, 18.7, 22.5, 28.5, 28.6, 31.3, 58.3, 65.2, 76.0, 86.7; HRMS (APPI, TOF) calcd for C<sub>11</sub>H<sub>20</sub>O (M<sup>+</sup>) 168.1514, found 168.1509.

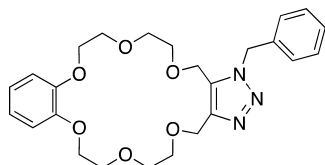
**General Procedure To Synthesize Triazole Adducts 1a and 5a–8a.** To a solution of alkyne 1 or 5–8 (0.10–0.30 mmol, 1 equiv) in CH<sub>3</sub>CN (1 M, in the case of 8, toluene was used) was added BnN<sub>3</sub> (10 equiv) and then the mixture heated to 80 °C for 48 h. In the case of 1 and 5, potassium trifluoromethanesulfonate (1 equiv) was added to facilitate the reaction. The reaction mixture was concentrated in vacuo and then purified by flash chromatography on silica gel.

**General Procedure for Kinetic Analysis.** Rates of cycloaddition with benzyl azide were obtained for the alkynyl crown ether 1 both in the presence and absence of potassium triflate using  $^1\text{H}$  NMR analysis with benzyl phenyl ether as an internal standard. A stock solution of

0.5 M benzyl azide containing 0.05 M benzyl phenyl ether internal standard was prepared in CD<sub>3</sub>CN along with 0.5 M stock solutions of the alkynes. Samples of each (0.5 mL) were added to an NMR tube which was then sealed with parafilm to afford a 1:1:0.1 (0.25:0.25:0.025 M) initial solution of azide/alkyne/standard. Formation of product over time was monitored relative to BnOPh standard at the given temperature.

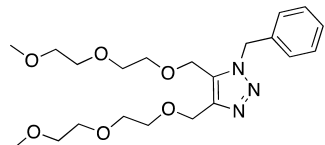
**General Procedure for Competition Experiments with the Alkynyl Crown Ether 1 and 1-K<sup>+</sup> and Various Alkynes 5–8.** To a solution of alkyne 1 (0.2 mmol, 1 equiv) and 5–8 (0.2 mmol, 1 equiv) in CD<sub>3</sub>CN (400 μL, 0.5 M) was added BnN<sub>3</sub> (0.2 mmol, 1 equiv) in a vial, and then the reaction mixture was transferred to an NMR tube. The reaction was heated to 80 °C for 48 h. In reactions in the presence of K<sup>+</sup>, potassium trifluoromethanesulfonate (1 equiv) was added to reaction mixture before addition of BnN<sub>3</sub>. The ratio of products was observed by <sup>1</sup>H NMR spectroscopy.

#### Triazole Adduct (1a).



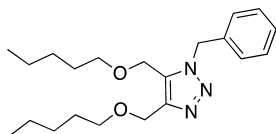
The resulting oil was purified by flash chromatography on silica gel (CHCl<sub>3</sub>, followed by 5% MeOH/CHCl<sub>3</sub>) to afford 38 mg (97% yield) of 1-benzyl-4,6,7,9,10,17,18,20,21,23-decahydro-1H-benzo[8,9]-[1,4,7,10,13,16]hexaoxacycloicosino[18,19-d][1,2,3]triazole (1a) as a solid: mp (MeOH/CHCl<sub>3</sub>) 37–38 °C; IR (neat)  $\nu_{\max}$  2920, 2868, 1593, 1499, 1454, 1355, 1327, 1255, 1220, 1122, 1092 cm<sup>-1</sup>; <sup>1</sup>H NMR (400 MHz)  $\delta$  3.54–3.61 (m, 4H), 3.64 (s, 4H), 3.71–3.73 (m, 4H), 4.04–4.07 (m, 4H), 4.56 (s, 2H), 4.57 (s, 2H), 5.55 (s, 2H), 6.88–6.92 (m, 4H), 7.23–7.36 (m, 5H); <sup>13</sup>C NMR (100 MHz)  $\delta$  52.7, 60.6, 64.3, 69.5, 69.6, 70.0, 70.4, 70.7, 70.9, 71.2, 71.5, 114.5, 114.8, 122.1, 122.2, 128.7, 129.0, 129.7, 133.32, 136.8, 144.4, 149.6, 149.7; HRMS (ESI<sup>+</sup>, TOF) calcd for C<sub>25</sub>H<sub>31</sub>N<sub>3</sub>O<sub>6</sub>Na (M + Na<sup>+</sup>) 492.2111, found 492.2107.

#### Triazole Adduct (5a).



The resulting oil was purified by flash chromatography on silica gel (CHCl<sub>3</sub>, followed by 5–10% MeOH/CHCl<sub>3</sub>) to afford 17 mg (27% yield) of 1-benzyl-4,5-bis((2-(2-methoxyethoxy)ethoxy)methyl)-1H-1,2,3-triazole 5a as a liquid: IR (neat)  $\nu_{\max}$  2872, 1456, 1348, 1246, 1199, 1094, 1026 cm<sup>-1</sup>; <sup>1</sup>H NMR (400 MHz)  $\delta$  3.35 (s, 3H), 3.56 (s, 3H), 3.50–3.67 (m, 16H), 4.50 (s, 2H), 4.67 (s, 2H), 5.63 (s, 2H), 7.25–7.35 (m, 5H); <sup>13</sup>C NMR (100 MHz)  $\delta$  52.5, 59.0, 60.2, 64.0, 69.4, 69.5, 70.3, 70.37, 70.4, 70.5, 71.8, 71.9, 127.7, 127.9, 128.2, 128.8, 131.7, 135.1; HRMS (ESI<sup>+</sup>, TOF) calcd for C<sub>21</sub>H<sub>33</sub>N<sub>3</sub>O<sub>6</sub>Na (M + Na<sup>+</sup>) 446.2267, found 446.2262.

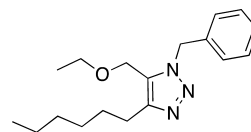
#### Triazole Adduct (6a).



The resulting oil was purified by flash chromatography on silica gel (5% to 50% EtOAc/Hexanes) to afford 63 mg (79% yield) of 1-benzyl-4,5-bis(pentyloxy)methyl-1H-1,2,3-triazole as colorless oil: IR (neat)  $\nu_{\max}$  2955, 2931, 2860, 1456, 1361, 1326, 1204, 1088, 1030, 1002 cm<sup>-1</sup>; <sup>1</sup>H NMR (400 MHz)  $\delta$  0.87–0.94 (m, 6H), 1.23–1.34 (m, 8H), 1.45–1.67 (m, 4H), 3.38 (t, J = 6.6 Hz, 2H), 3.47 (t, J = 6.6 Hz, 2H), 4.51 (s, 2H), 4.55 (s, 2H), 5.58 (s, 2H), 7.25–7.39 (m, 5H); <sup>13</sup>C NMR (100 MHz)  $\delta$  14.36, 14.39, 23.19, 23.21, 29.0, 29.2, 29.9, 30.1, 52.8, 60.5, 64.1, 71.0, 71.4, 128.6, 129.0, 129.7, 133.3, 136.9,

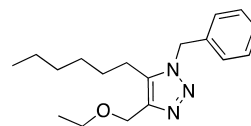
144.5; HRMS (CI<sup>+</sup>, TOF) calcd for C<sub>21</sub>H<sub>34</sub>N<sub>3</sub>O<sub>2</sub> (M + H<sup>+</sup>) 360.2651, found 360.2657.

#### Triazole Adduct (7a1).



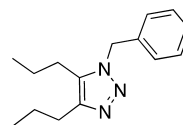
The resulting oil was purified by flash chromatography on silica gel (5% → 25% → 50% EtOAc/hexanes) to afford two separable regioisomers. 1-Benzyl-5-(ethoxymethyl)-4-hexyl-1H-1,2,3-triazole 7a1 (29 mg, 32% yield): colorless oil; IR (neat)  $\nu_{\max}$  2928, 2857, 1497, 1456, 1377, 1205, 1092, 1012 cm<sup>-1</sup>; <sup>1</sup>H NMR (400 MHz)  $\delta$  0.86 (t, J = 6.8 Hz, 3H), 1.14 (t, J = 7.0 Hz, 3H), 1.26–1.34 (m, 6H), 1.67 (pentet, J = 7.5 Hz, 2H), 3.37 (q, J = 7.0 Hz, 2H), 4.29 (s, 2H), 5.57 (s, 2H), 7.20 (d, J = 7.9 Hz, 2H), 7.27–7.33 (m, 3H); <sup>13</sup>C NMR (100 MHz)  $\delta$  13.9, 14.8, 22.4, 24.9, 28.8, 29.7, 31.4, 52.3, 59.7, 65.7, 127.3, 128.0, 128.7, 129.1, 135.1, 147.1; HRMS (CI<sup>+</sup>, TOF) calcd for C<sub>18</sub>H<sub>28</sub>N<sub>3</sub>O (M + H<sup>+</sup>) 302.2246, found 302.2236.

#### Triazole Adduct (7a2).



1-Benzyl-4-(ethoxymethyl)-5-hexyl-1H-1,2,3-triazole (7a2) (20 mg, 22% yield) as a colorless oil: IR (neat)  $\nu_{\max}$  2929, 2859, 1496, 1456, 1379, 1328, 1233, 1094 cm<sup>-1</sup>; <sup>1</sup>H NMR (400 MHz)  $\delta$  0.84 (t, J = 6.8 Hz, 3H), 1.16–1.38 (m, 11H), 2.57 (t, J = 7.8 Hz, 3H), 3.50 (q, J = 7.0 Hz, 2H), 4.57 (s, 2H), 5.48 (s, 2H), 7.17 (d, J = 7.4 Hz, 2H), 7.28–7.34 (m, 3H); <sup>13</sup>C NMR (100 MHz)  $\delta$  13.8, 15.0, 22.3, 22.6, 28.4, 28.8, 31.2, 51.8, 63.6, 65.5, 127.0, 128.1, 128.8, 135.0, 135.9, 142.3; HRMS (CI<sup>+</sup>, TOF) calcd for C<sub>18</sub>H<sub>28</sub>N<sub>3</sub>O (M + H<sup>+</sup>) 302.2236, found 302.2232.

#### Triazole Adduct (8a).



The resulting oil was purified by flash chromatography on silica gel (5% to 50% EtOAc/hexanes) to afford 70 mg (83% yield) of 1-benzyl-4,5-dipropyl-1H-1,2,3-triazole (8a) as a colorless oil: IR (neat)  $\nu_{\max}$  2955, 2931, 2860, 1456, 1361, 1326, 1204, 1088, 1030, 1002 cm<sup>-1</sup>; <sup>1</sup>H NMR (400 MHz)  $\delta$  0.85 (t, J = 7.4 Hz, 3H), 0.96 (t, J = 7.4 Hz, 3H), 1.36 (sextet, J = 6.0 Hz, 2H), 1.68 (sextet, J = 6.0 Hz, 2H), 2.55 (t, J = 7.7 Hz, 2H), 2.58 (t, J = 7.6 Hz, 2H), 5.49 (s, 2H), 7.19 (d, J = 7.7 Hz, 2H), 7.30–7.38 (m, 3H); <sup>13</sup>C NMR (100 MHz)  $\delta$  14.0, 14.2, 23.0, 23.7, 24.9, 27.7, 52.1, 128.1, 128.9, 129.8, 134.3, 137.5, 145.8; HRMS (CI<sup>+</sup>, TOF) calcd for C<sub>15</sub>H<sub>22</sub>N<sub>3</sub> (M + H<sup>+</sup>) 244.1814, found 244.1811.

## ■ ASSOCIATED CONTENT

### 📄 Supporting Information

Geometries, energies, and imaginary frequencies (TSs) for all reactants, products and transition states, 1D and 2D NMR of all synthetic intermediates, and products. This material is available free of charge via the Internet at <http://pubs.acs.org>.

## ■ AUTHOR INFORMATION

### Corresponding Authors

\*E-mail: [gududley@chem.fsu.edu](mailto:gududley@chem.fsu.edu).

\*E-mail: [alabugin@chem.fsu.edu](mailto:alabugin@chem.fsu.edu).

### Notes

The authors declare no competing financial interest.

## ACKNOWLEDGMENTS

I.A. and G.D. are grateful to the National Science Foundation (Grants CHE-1152491 and CHE-1300722) for support of this research project.

## REFERENCES

- (1) (a) Kolb, H. C.; Finn, M. G.; Sharpless, B. K. *Angew. Chem., Int. Ed.* **2001**, *40*, 2004. (b) Finn, M. G.; Fokin, V. V., Guest Eds. *Chem. Soc. Rev.* **2010**, *39*, 1221.
- (2) (a) Tron, G. C.; Pirali, T.; Billington, R. A.; Canonico, P. L.; Sorba, G.; Genazzani, A. A. *Med. Res. Rev.* **2008**, *28*, 278. (b) Su, Y.; Ge, J.; Zhu, B.; Zheng, Y.-G.; Zhu, Q.; Yao, S. Q. *Curr. Opin. Chem. Biol.* **2013**, *17*, 768.
- (3) (a) Jewett, J. C.; Bertozzi, C. R. *Chem. Soc. Rev.* **2010**, *39*, 1272. (b) Ning, X.; Guo, J.; Wolfert, M.; Boons, G.-J. *Angew. Chem., Int. Ed.* **2008**, *47*, 2253.
- (4) Binder, W. H.; Sachsenhofer, R. *Macromol. Rapid Commun.* **2007**, *28*, 15.
- (5) Huang, S.; Clark, R. J.; Zhu, L. *Org. Lett.* **2007**, *9*, 4999.
- (6) Golas, P. L.; Tsarevsky, N. V.; Sumerlin, B. S.; Matyjaszewski, K. *Macromolecules* **2006**, *39*, 6451.
- (7) (a) Bertozzi, C. R. *Curr. Opin. Chem. Biol.* **2013**, *17*, 717. (b) Borrmann, A.; van Hest, J. C. M. *Chem. Sci.* **2014**, *5*, 2123. (c) Sletten, E. M.; Bertozzi, C. R. *Angew. Chem., Int. Ed.* **2009**, *48*, 6974. (d) Chang, P. V.; Bertozzi, C. R. *Chem. Commun.* **2012**, *48*, 8864.
- (8) (a) Hein, J. E.; Fokin, V. V. *Chem. Soc. Rev.* **2010**, *39*, 1302. (b) Tornøe, C. W.; Meldal, M. *Chem. Rev.* **2008**, *108*, 2952. (c) Moses, J. E.; Moorhouse, A. D. *Chem. Soc. Rev.* **2007**, *36*, 1249.
- (9) Rostovtsev, V. V.; Green, L. G.; Fokin, V. V.; Sharpless, K. B. *Angew. Chem., Int. Ed.* **2002**, *41*, 2596.
- (10) Tornøe, C. W.; Christensen, C.; Meldal, M. *J. Org. Chem.* **2002**, *67*, 3057.
- (11) Huisgen, R. *1,3-Dipolar Cycloadditions—Introduction, Survey, Mechanism. In 1,3-Dipolar Cycloaddition Chemistry*; Padwa, A., Ed.; Wiley: New York, 1984; pp 1–176.
- (12) The toxicity of Cu salts can be significantly alleviated by a suitable choice of Cu-coordinating ligands: Hong, V.; Steinmetz, N. F.; Manchester, M.; Finn, M. G. *Bioconjugate Chem.* **2010**, *21*, 1912.
- (13) Bernardin, A.; Cazet, A.; Guyon, L.; Delannoy, P.; Vinet, F.; Bonnaffé, D.; Texier, I. *Bioconjugate Chem.* **2010**, *21*, 583.
- (14) Han, H.-S.; Devaraj, N. K.; Lee, J.; Hilderbrand, S. A.; Weissleder, R.; Bawendi, M. G. *J. Am. Chem. Soc.* **2010**, *132*, 7838.
- (15) Codelli, J. A.; Baskin, J. M.; Agard, N. J.; Bertozzi, C. R. *J. Am. Chem. Soc.* **2008**, *130*, 11486.
- (16) (a) Poloukhine, A. A.; Mbua, N. E.; Wolfert, M. A.; Boons, G.-J.; Popik, V. V. *J. Am. Chem. Soc.* **2009**, *131*, 15769. (b) Sanders, B. C.; Friscourt, F.; Ledin, P. A.; Mbua, N. E.; Arumugam, S.; Guo, J.; Boltje, T. J.; Popik, V. V.; Boons, G.-J. *J. Am. Chem. Soc.* **2011**, *133*, 949.
- (17) (a) Dommerholt, J.; Schmidt, S.; Temming, R.; Hendricks, L. J. A.; Rutjes, F. P. J. T.; van Hest, J. C. M.; Lefeber, D. J.; Friedl, P.; van Delft, F. L. *Angew. Chem., Int. Ed.* **2010**, *49*, 9422. (b) Becer, C. R.; Hoogenboom, R.; Schubert, U. S. *Angew. Chem., Int. Ed.* **2009**, *48*, 4900. (c) Varga, B. R.; Kállay, M.; Hegyi, K.; Béni, S.; Kele, P. *Chem.—Eur. J.* **2012**, *18*, 822. (d) Debets, M. F.; van Berkel, S. S.; Schoffelen, S.; Rutjes, F. P. J. T.; van Hest, J. C. M.; van Delft, F. L. *Chem. Commun.* **2010**, *46*, 97. (e) Kuzmin, A.; Poloukhine, A.; Wolfert, M. A.; Popik, V. V. *Bioconjugate Chem.* **2010**, *21*, 2076. (f) Manova, R.; van Beek, T. A.; Zuilhof, H. *Angew. Chem., Int. Ed.* **2011**, *50*, 5428.
- (18) Wittig, G.; Krebs, A. *Chem. Ber.* **1961**, *94*, 3260.
- (19) Agard, N. J.; Prescher, J. A.; Bertozzi, C. R. *J. Am. Chem. Soc.* **2004**, *126*, 15046; Corrected rate constants: *J. Am. Chem. Soc.* **2005**, *127*, 11196.
- (20) Chang, P. V.; Prescher, J. A.; Sletten, E. M.; Baskin, J. M.; Miller, I. A.; Agard, N. J.; Lo, A.; Bertozzi, C. R. *Proc. Natl. Acad. Sci. U.S.A.* **2010**, *107*, 1821.
- (21) (a) Swarts, B. M.; Holsclaw, C. M.; Jewett, J. C.; Alber, M.; Fox, D. M.; Siegrist, M. S.; Leary, J. A.; Kalscheuer, R.; Bertozzi, C. R. *J. Am. Chem. Soc.* **2012**, *134*, 16123. (b) Beahm, B. J.; Dehnert, K. W.; Derr, N. L.; Kuhn, J.; Eberhart, J. K.; Spillmann, D.; Amacher, S. L.; Bertozzi, C. R. *Angew. Chem., Int. Ed.* **2014**, *53*, 3347. (c) Beladri, B.; de la Zerda, A.; Spicciarich, D. R.; Maund, S. L.; Peehl, D. M.; Bertozzi, C. R. *Angew. Chem., Int. Ed.* **2013**, *52*, 14045.
- (22) Jewett, J. C.; Sletten, E. M.; Bertozzi, C. R. *J. Am. Chem. Soc.* **2010**, *132*, 3688. See also: Jewett, J. C.; Bertozzi, C. R. *Org. Lett.* **2011**, *13*, 5937.
- (23) Reactant destabilization has been also used to activate alkynes in cycloaromatization reactions: (a) Nicolaou, K. C.; Zuccarello, G.; Ogawa, Y.; Schweiger, E. J.; Kumazawa, T. *J. Am. Chem. Soc.* **1988**, *110*, 4866. (b) Nicolaou, K. C.; Smith, A. L. *Acc. Chem. Res.* **1992**, *25*, 497. (c) Magnus, P.; Carter, P.; Elliott, J.; Lewis, R.; Harling, J.; Pitterna, T.; Bauta, W. E.; Fortt, S. *J. Am. Chem. Soc.* **1992**, *114*, 2544. (d) Snyder, J. P. *J. Am. Chem. Soc.* **1990**, *112*, 5367. (e) Semmelhack, M. F.; Neu, T.; Foubelo, F. J. *Org. Chem.* **1994**, *59*, 5038. (f) Schreiner, P. R. *J. Am. Chem. Soc.* **1998**, *120*, 4184. (g) Schreiner, P. R. *Chem. Commun.* **1998**, 483. (h) Mita, T.; Kawata, S.; Hirama, M. *Chem. Lett.* **1998**, 959. (i) Alabugin, I. V.; Manoharan, M. *J. Phys. Chem. A* **2003**, *107*, 3363. (j) Mohamed, R. K.; Peterson, P. W.; Alabugin, I. V. *Chem. Rev.* **2013**, 7089. For the analysis of electronic consequences of strain, see: (k) Tykwinski, R. R. *Chem. Commun.* **1999**, 905. For the contrasting effects of strain in alkyne cyclizations, see: (l) Alabugin, I. V.; Manoharan, M. *J. Am. Chem. Soc.* **2005**, *127*, 12583. (m) Alabugin, I. V.; Manoharan, M. *J. Am. Chem. Soc.* **2005**, *127*, 9534. (n) Gilmore, K.; Alabugin, I. V. *Chem. Rev.* **2011**, *111*, 6513.
- (24) Baskin, J. M.; Prescher, J. A.; Laughlin, S. T.; Agard, N. J.; Chang, P. V.; Miller, I. A.; Lo, A.; Codelli, J. A.; Bertozzi, C. R. *Proc. Natl. Acad. Sci. U.S.A.* **2007**, *104*, 16793.
- (25) (a) Ess, D. H.; Jones, G. O.; Houk, K. N. *Org. Lett.* **2008**, *10*, 1633. (b) Schoenebeck, F.; Ess, D. H.; Jones, G. O.; Houk, K. N. *J. Am. Chem. Soc.* **2009**, *131*, 8121. See also: (c) Chenoweth, K.; Chenoweth, D.; Goddard, W. A., III. *Org. Biomol. Chem.* **2009**, *7*, 5255. (d) Bach, R. D. *J. Am. Chem. Soc.* **2009**, *131*, 5233.
- (26) Gold, B.; Schevchenko, N.; Bonus, N.; Dudley, G. B.; Alabugin, I. V. *J. Org. Chem.* **2012**, *77*, 75.
- (27) This effect is similar to the electronic origin of torquoselectivity in electrocyclic reactions, where similar interactions provide selective stabilization to the TS because of the increased donor and acceptor ability of chemical bonds upon their distortion and breaking. (a) Dolbier, W. R., Jr.; Koroniak, H.; Houk, K. N.; Sheu, C. *Acc. Chem. Res.* **1996**, *29*, 471. (b) Kirmse, W.; Rondan, N. G.; Houk, K. N. *J. Am. Chem. Soc.* **1984**, *106*, 7989.
- (28) Gordon, C. G.; Mackey, J. L.; Jewett, J. C.; Sletten, E. M.; Houk, K. N.; Bertozzi, C. R. *J. Am. Chem. Soc.* **2012**, *134*, 9199.
- (29) Ess, D. H.; Houk, K. N. *J. Am. Chem. Soc.* **2008**, *130*, 10187.
- (30) A recent report has suggested Hartree–Fock LUMO energies can be used as a tool for predicting the reactivity of alkyne in SPAAC: Garcia-Hartjes, J.; Dommerholt, J.; Wennekes, T.; van Delft, F. L.; Zuilhof, H. *Eur. J. Org. Chem.* **2013**, 3712.
- (31) For azide substituent effects on FMO interactions see: Muller, M.; Maichle-Mossmar, C.; Bettinger, H. F. *J. Org. Chem.* **2014**, *79*, 5478.
- (32) Gold, B.; Dudley, G. B.; Alabugin, I. V. *J. Am. Chem. Soc.* **2013**, *135*, 1558.
- (33) This may be the case in the recent report of difluorocyclononyne: Sletten, E. M.; Almeida, G. d.; Bertozzi, C. R. *Org. Lett.* **2014**, *16*, 1634.
- (34) (a) Kihara, N.; Kiboda, K. *Org. Lett.* **2009**, *11*, 1313. (b) Kotha, S.; Waghule, G. T. *J. Org. Chem.* **2012**, *77*, 6314.
- (35) For a recent use of DCC in radical reactions, see: Mondal, S.; Mohamed, R. K.; Manoharan, M.; Phan, H.; Alabugin, I. V. *Org. Lett.* **2013**, *15*, 5650.
- (36) The entropy of activation of  $-15.9$  cal/mol·K for  $1-K^+$  is relatively low for an azide/alkyne cycloaddition. In our previous report of electronically activated alkynes, activation entropies ranged from  $-15.7$  to  $-19.0$  cal/mol·K for the more reactive alkynes investigated where H-bonding interactions led to a more ordered TS (see ref 26).



(37) Frisch, M. J. et al. *Gaussian 09, Revision B.01*; Gaussian: Wallingford, CT, 2009.

(38) Ess, D. H.; Houk, K. N. *J. Phys. Chem. A* **2005**, *109*, 9542.

(39) Burns, L. A.; Vazquez-Mayagoitia, A.; Sumpter, B. G.; Sherrill, C. D. *J. Chem. Phys.* **2011**, *134*, 084107.

(40) (a) Miertuš, S.; Scrocco, E.; Tomasi, J. *J. Chem. Phys.* **1981**, *55*, 117. (b) Cossi, M.; Rega, N.; Scalmani, G.; Barone, V. *J. Comput. Chem.* **2003**, *24*, 669.

(41) NBO 4.0. Glendening, E. D.; Badenhoop, J. K.; Reed, A. E.; Carpenter, J. E.; Weinhold, F. Theoretical Chemistry Institute, University of Wisconsin, Madison, WI, 1996.

(42) For selected examples, see: (a) Alabugin, I. V.; Manoharan, M.; Peabody, S.; Weinhold, F. *J. Am. Chem. Soc.* **2003**, *125*, 5973.

(b) Alabugin, I. V.; Manoharan, M. *J. Org. Chem.* **2004**, *69*, 9011.

(c) Vasilevsky, S. F.; Mikhailovskaya, T. F.; Mamatyuk, V. I.; Bogdanchikov, G. A.; Manoharan, M.; Alabugin, I. V. *J. Org. Chem.* **2009**, *74*, 8106. (d) Mondal, S.; Gold, B.; Mohamed, R. K.; Alabugin, I. V. *Chem—Eur. J.* **2014**, DOI: 10.1002/chem.201402843.

(43) Reed, A. E.; Curtiss, L. A.; Weinhold, F. *Chem. Rev.* **1988**, *88*, 899.

(44) Previously, we have shown that the hyperconjugative energies estimated by second order perturbation and deletion approaches agree well with each other. Alabugin, I. V.; Zeidan, T. A. *J. Am. Chem. Soc.* **2002**, *124*, 3175.

(45) (a) Weinhold, F. *Encyclopedia of Computational Chemistry*; Schleyer, P. v. R., Ed.; John Wiley & Sons: New York, 1998; Vol 3, p 1972. (b) See also: [www.chem.wisc.edu/~nbo5](http://www.chem.wisc.edu/~nbo5) (accessed June 19, 2014).

(46) Reed, A. E.; Weinhold, F. *J. Chem. Phys.* **1985**, *83*, 1736.

(47) The recently reported nine-membered 3-aza-5-[7]orthocyclophene contains an alkyne moiety bent to a much greater degree (164–166°): Igawa, K.; Kawabata, T.; Ni, R.; Tomooka, K. *Chem. Lett.* **2013**, *42*, 1374. This distortion of 160° should correspond to destabilization of 8.1 kcal/mol for 2-butyne, lowered to 7.3 kcal/mol with a single C–F propargylic acceptor.<sup>26</sup> While the propargylic C–N bond should provide stabilization to the bent alkyne, much larger effects should be present in the TS (see Figure 8), providing access to alkynes that can benefit from both strain activation and TS stabilization. For the expansion of this work toward the preparation of a variety of medium-sized cyclic alkynes with endocyclic heteroatoms, see: Ni, R.; Igawa, K.; Tomooka, K. *Abstracts of Papers, 93rd Annual Meeting of The Chemical Society of Japan, Kusatsu*; The Chemical Society of Japan: Tokyo, 2013; pp 1E6–49.

(48) HOMO (azide) refers to the highest energy in-plane azide orbital. Reference 25b has shown the analogous out of plane orbital to be the HOMO and the in-plane to be the HOMO-1.

(49) The latter interaction is surprising because azide and potassium are separated by the alkyne. We will investigate the origin of these computational effects in our future work.

(50) However, distortion energies of crown alkynes are higher than that for the highly bent cyclooctyne molecule.

(51) Cannizzo, C.; Mazaleyrat, J.-P.; Melandri, F.; Wakselman, M.; Wright, K. *Tetrahedron* **2002**, *58*, 5811.

(52) Byun, J.; Gross, M. L.; George, M.; Kamzelski, A. Z.; Parees, D. M.; Swijter, D. F. H.; Willcox, D. A.; Swijter, D. F. H. *J. Mass Spectrom.* **1997**, *32*, 71.

(53) Barbot, F.; Dauphin, B.; Miginiac, P. *Synthesis* **1985**, *8*, 768.